



Modelling the kinetics of coagulation process for tannery industry effluent treatment using *Moringa oleifera* seeds protein

Marichamy Mageshkumar^{a,*}, Ramasamy Karthikeyan^b

^aDepartment of Chemical Engineering, School of Bio Engineering, SRM University, Kattankulathur 603 203, Tamil Nadu, India, Tel. +91 9940585262; email: mmagesh23@gmail.com

^bDepartment of Chemical Engineering, Anjalai Ammal Mahalingam Engineering College, Kovilvenni, Thiruvavur, Tamil Nadu, India, Tel. +91 9940561915; email: drkarthi@yahoo.com

Received 3 April 2015; Accepted 30 June 2015

ABSTRACT

The ability of the natural coagulant extracted from *Moringa oleifera* seeds to remove the turbidity from tannery industry wastewater was studied. Coagulation experiments were performed using conventional jar test apparatus with 4–9 pH range and coagulant dose ranging from 10 to 50 mL. The active coagulation component of *M. oleifera* seed was prepared separately using NaCl and KCl salt solutions. Turbidity removal efficiency of NaCl-extracted coagulant and KCl-extracted coagulant was compared. The turbidity of raw tannery wastewater was reduced from 121.9 to 29.01 mg/L at an optimum pH 7 and coagulant dosage of 40 mL. The maximum turbidity removal efficiency was observed as 76.2 and 71.2% for NaCl- and KCl-extracted coagulants, respectively. The coagulation kinetic study suggested that the process follows second-order kinetics for both type coagulants, and the parameters for rate equation were obtained from the regression equations.

Keywords: Tannery industry wastewater; *Moringa oleifera* coagulant (MOC); Turbidity removal; Coagulation kinetics; Particle size distribution

1. Introduction

In most developing countries of the world, industrial effluents are usually discharged into adjacent land or river. A tannery industry effluent contains a number of substances that are deleterious to the environment. Tannery industry can create heavy pollution from effluents containing high levels of salinity, organic loading, inorganic matter, dissolved and suspended solids [1]. This industry uses large quantities of water and, in turn, produces large quantities of liquid effluents [2]. The World Health Organization

(WHO) has stipulated safe limits for the discharge of tannery effluents into the environment. The treatment of tannery wastewater has been studied using various analytical techniques, namely ozonation, reverse osmosis, adsorption, electrochemical oxidation and coagulation process [3]. Coagulation is a process developed for the removal of colloidal particles and suspended impurities from wastewater. The removal of fine suspended impurities by gravity settling is very slow because the buoyant force acting on the particles overrules the force of gravity [4]. In coagulation process, stable colloidal particles are destabilized in suspension, such that they can agglomerate into settleable flocs. Aluminium- and iron cation-related

*Corresponding author.

compounds are the commonly used coagulants in water treatment units. These coagulants are inorganic in nature and affect the pH of the treated water, which can create secondary contamination. Further, residual aluminium ion in treated water has been linked to Alzheimer disease. Synthetic organic polymers together with aluminium and iron salts are also used as coagulant. The major problem with polymer-based coagulant is its non-biodegradability after it was disposed along with sludge. Chemical-based coagulants are often expensive and in many countries they have to be imported. Commercially available coagulant aids such as poly aluminium chloride and ferric chloride are effective in treatment, but disposal of sludge generated is not economical and environmentally detrimental. There is an urgent need to replace these synthetic chemicals with natural coagulants which are cost-effective and environment-friendly. It is therefore desired to substitute chemical coagulants with plant-based coagulants to prevent the above-mentioned drawbacks.

The advantages of using natural plant-based coagulants are as follows: cheaper than chemical-based coagulants, acceptable pH of treated water and biodegradable sludge. Natural coagulants are mostly either polysaccharides or proteins [5]. The four commonly used plant-based coagulants in water treatment units are *Moringa oleifera* seeds, *Strychnos potatorum*, *Cactus opuntia* [6] and tannin. Nopal cladode (*C. opuntia*) is mainly used to remove turbidity from synthetic wastewater [7]. Pre-treatment of winery wastewater and olive mill wastewater using chitosan as a natural coagulant showed best performance at the actual pH of wastewater [8]. *S. potatorum* extract is an anionic polyelectrolyte that removes turbidity by means of interparticle bridging. Adsorption sites which are responsible for bridging are weak, and hence, the floc growth is affected during coagulation. This reduces the turbidity removal efficiency of *S. potatorum* coagulant. Polygalacturonic acid present in *Cactus* species is possibly the active ingredient responsible for coagulation. The polymeric acid is anionic due to partial deprotonation of the carboxylic functional group in aqueous solution. The presence of –OH group along its polymeric chain may distort the linearity of the chain and hinder the formation of stable flocs. Zimmerman reports that the coagulation capability of *Cactus* accounts for only 50% of turbidity removal [9]. In most of the effluents, suspended particles which are responsible for turbidity are negatively charged particles. *M. oleifera* seed coagulant acts as a source of cationic polyelectrolytes and involves in electrostatic interaction with impurity particles to form

large size stable flocs which settles easily. The above data suggest that the coagulation efficiency of *M. oleifera* seed extract is high and show better performance on comparing with other natural coagulants.

Our study explains the potential application of protein coagulant extracted from *M. oleifera* seeds through a salt solution for tannery wastewater treatment. *M. oleifera* is a tropical plant belonging to the family moringaceae, which is a family of shrubs with 14 known species. *M. oleifera* is native to India, but is now found throughout the tropics. This multipurpose tree helps to clean dirty water and is a useful source of medicine [10]. *M. oleifera* coagulant (MOC) was used in raw industrial effluents and synthetic turbid waters for turbidity removal in the range of 80–90% [11]. The coagulant activity of the seeds is mainly due to the inherent positive charged protein produced in aqueous medium. These proteins are cationic dimmers which have a molecular mass of approximately 13 KDa and isoelectric pH value of 10 and 11, respectively [12]. In coagulation, when MOC is used, the sludge volume index is less compared to alum and sludge disposal problem is minimum [13]. The cultivation cost of producing 1 kg (3,400 seeds) of *M. oleifera* is approximately US\$2 [14]. The present market price of dried seeds is about US\$ 20 per kg. Previous researchers documented the usage of aluminium sulphate for coagulation process to remove C.I. Acid Black 210 dye from industrial grade leather processing effluent [15] and turbidity removal from tannery wastewater [16]. *M. oleifera* as primary coagulant was used successfully for the treatment of raw distillery spent wash [17] and removal of long-chain anionic surfactants in aqueous solution [18]. Although there are many studies been carried out on *M. oleifera* as a coagulant for treating surface water and other raw industrial water, studies on the treatment of tannery wastewater by *M. oleifera* coagulant and kinetics of coagulation process have not been reported. Thus, this study is aimed to examine the efficiency of MOC towards tannery wastewater treatment and establishing the coagulation kinetics.

Thus, *M. oleifera* seed protein is a suitable natural coagulant for tannery wastewater treatment. This coagulant may be a move towards a water treatment method which is cheaper and biodegradable, easy to handle. The aim of our research was to study the ability of the natural coagulant obtained from *M. oleifera* seeds to treat the wastewater collected from leather processing industry. This study also focuses on predicting the kinetic parameters and model equations of the coagulation process.

2. Theory of coagulation kinetics

The kinetics of coagulation process is modelled by the equation of the form:

$$\frac{-dC}{dt} = kC^n \quad (1)$$

where “ C ” is the mass of particles per litre, “ t ” is the coagulation time, “ k ” is the n th order rate constant and “ n ” is the order of the coagulation process. The negative sign represents the fact turbidity concentration decreases as a function of increasing time (t). The process rate constant is a result of collision efficiency E multiplied with the Smoluchowski rate constant for rapid coagulation K_{RC} [19].

$$k = EK_{RC} \quad (2)$$

The rapid coagulation rate constant is given by,

$$K_{RC} = \frac{4k_B T}{3\mu} \quad (3)$$

where k_B is the Boltzmann constant, T is the absolute temperature and μ is the viscosity of the fluid. Eq. (2) gives the following expression of collision efficiency.

$$E = \frac{k}{K_{RC}} \quad (4)$$

The relationship between friction factor and n th order coagulation rate constant has been reported to be [20].

$$\beta = 2k \quad (5)$$

An expression for Brownian diffusion coefficient (D) due to concentration gradient has been shown to be:

$$D = \frac{k_B T}{\beta} \quad (6)$$

For a first-order ($n = 1$) coagulation process, the rate equation is shown as,

$$\frac{-dC}{dt} = k_1 C \quad (7)$$

Eq. (7) upon integration yields,

$$\ln\left(\frac{C_0}{C}\right) = k_1 t \quad (8)$$

where C_0 is initial turbidity in mg/L, C is particle density at time “ t ” and k_1 is the first-order rate constant in (1/min). Eq. (8) shows that the plot of $\ln(C_0/C)$ along Y -axis and time (t) along X -axis should be a straight line passes through the origin and the line slope equivalent to k_1 .

If the process follows, second-order kinetics ($n = 2$), rate expression in differential form for coagulation process should be written as follows:

$$\frac{-dC}{dt} = k_2 C^2 \quad (9)$$

where k_2 is second-order rate constant in L/(mg min). After integration and simplification, the second-order rate equation in integral form is written as follows:

$$\frac{1}{C} = k_2 t + \frac{1}{C_0} \quad (10)$$

Eq. (10) implies a straight line with slope k_2 and intercept made by the line along the Y -axis is $\ln(1/C_0)$ because the equation resembles slope-intercept form of straight line. The turbidity concentration obtained through experimental runs is plotted using Eqs. (8) and (10). When the time vs. concentration term plot (straight line) pass through origin, it is concluded coagulation follows first-order kinetics. If the plot resembles a straight line which does have slope and Y -axis intercept, then the process fits second-order kinetic model. One of the important time scales for the identification of the early stages in the coagulation process is the half-life period ($t_{1/2}$). It is defined as the time needed for the initial turbidity to drop to one-half the original turbidity concentration [21]. For first-order coagulation process, half-life period is shown by,

$$(t_{1/2})_{I\text{order}} = \frac{0.6931}{k_1} \quad (11)$$

Similarly for second-order process, half-life period is calculated by,

$$(t_{1/2})_{II\text{order}} = \frac{1}{k_2 C_0} \quad (12)$$

This time parameter is helpful to calculate the kinetic parameters of the rate expression for coagulation process, viz. process order (n) and rate constant (k).

The particle distribution plot for coagulation as function of time can be generally represented as follows:

$$N_m(t) = 4N_0^m(kt)^{m-1}(2 + kN_0t)^{-(m+1)} \quad (13)$$

For monomer $m = 1$, dimer $m = 2$ and trimer $m = 3$, respectively.

3. Materials and methods

3.1. Tannery industry wastewater

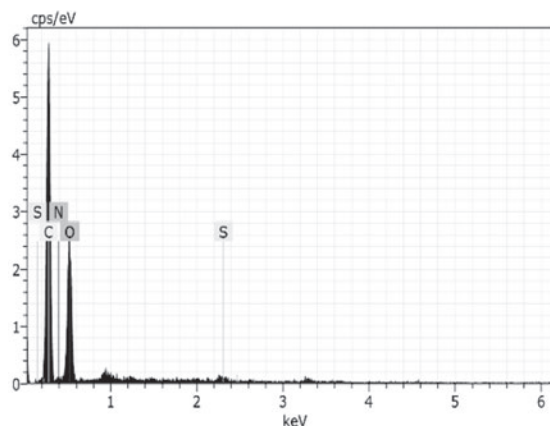
The untreated effluent of the tannery processing industry (real effluent) was collected from the equalization tank of the common effluent treatment plant located near Chennai city, Tamil Nadu state, India. The physico-chemical properties of the effluent were determined based on the standard methods [22] and presented in Table 1.

3.2. *M. oleifera* seed powder characterization

The characterization of seed powder was used to identify the functional groups and the elements present. Fig. 1 shows the energy-dispersive X-ray spectroscopy (EDS) analysis of dry *M. oleifera* seed powder. The presence of basic elements such as carbon, hydrogen and oxygen in large proportion confirmed the organic nature of the powder, which accounts for the biodegradability of seed coagulant. The elemental composition of the seed powder was as follows: C-61.38%, O-34.91%, N-3.46% and S-0.25%. With only one atom of each in the molecular formula for this compound, the ratios, based on weight % determined by analysis, are correct within a reasonable margin of error. Fig. 2. shows the Fourier transform infrared spectroscopy (FTIR) spectrum for raw seed powder. The vibration of amine group and water molecule was confirmed with the intense band stretch occurring at $3,306.80 \text{ cm}^{-1}$. The peak at $2,921.86 \text{ cm}^{-1}$ was due to the presence of C-H alkyl type of bond. Sharp peak at the bend $1,542.59 \text{ cm}^{-1}$ confirms the presence of aromatic groups possessing C=C type of bond. Strong stretch at the peak $1,057.59 \text{ cm}^{-1}$

Table 1
Physico-chemical characteristics of raw tannery wastewater sample

Parameter	Magnitude
pH	8.2 ± 0.4
COD	$3,500 \pm 400 \text{ mg/L}$
Chromium	$22 \pm 3 \text{ mg/L}$
Turbidity	121.9 mg/L
TDS	$19,500 \pm 300 \text{ mg/L}$
Colour	Dark green



Element	Atomic number	Series	Atom %	Error weight %
C	6	K - series	61.38	7.62
O	8	K - series	34.91	6.51
N	7	K - series	3.46	1.47
S	16	K - series	0.25	0.08

Fig. 1. EDS image of native *M. oleifera* seed powder.

confirms the presence of aliphatic amines with C=N type bond. Many peaks formed from 590 to 440 cm^{-1} confirm the presence of halogenated alkanes. Presence of carboxylic acid R-COOH is confirmed by strong, very broad spectrum at $2,500 \text{ cm}^{-1}$. Scanning electron microscopy (SEM) image was taken to study the surface topography of sample. Average particle size for the powder is $200 \mu\text{m}$. Fibre nature of the seeds was observed through detailed analysis of image (Fig. 3).

3.3. *M. oleifera* seed coagulant

Dehydrated seeds were collected from rural areas in the northern part of Tamil Nadu, India. The unsheathing of seeds was performed in the following manner. Husk removed seeds were made into powder by electric blender. Sodium chloride (0.25 M) and potassium chloride (0.25 M) salt solutions were prepared. Five grams of *M. oleifera* seed powder was added to 100 mL of each salt solution in separate beakers (concentrated solution was so considered 5%/w/w) and stirred at room temperature for 15 min using a magnetic stirrer. The extract was then filtered, and the milky liquid-like filtrate was used as coagulant for water treatment. *M. oleifera* seed coagulant prepared in this way was used on the same day due to avoid decrease in coagulant activity [23].

3.4. Coagulation experiment procedure

Tannery effluent samples were diluted to 10% of their initial concentration, and the diluted samples

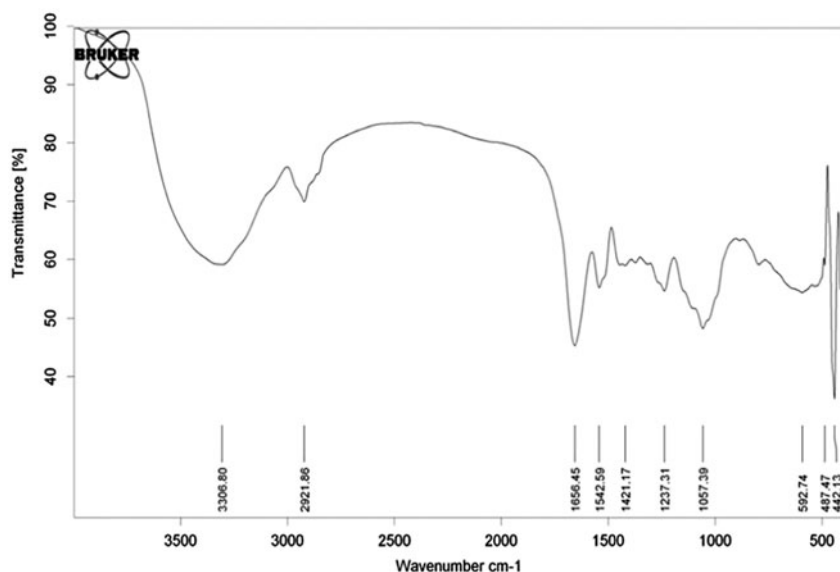


Fig. 2. Functional group and chemical bond analysis of seed powder using FTIR.

were then used for further analysis. The pH of the sample was adjusted using 0.5 N H_2SO_4 or 0.5 N NaOH solution as required.

Coagulation experiments were conducted using the conventional jar test apparatus. The 1,000 mL beakers (six in number) were filled with 500 mL of tannery industry wastewater. The extracted coagulant dosage added to each beaker varied from 10 to 50 mL. The specimens were agitated at 150 rpm for 3 min (rapid mixing) and then at 30 rpm for 30 min (slow mixing). The contents of each beaker were then allowed to accumulate with the settling time of 30 min [24]. The above procedure was performed using both NaCl- and KCl-extracted coagulant and the performance in terms of % turbidity removal was compared. The supernatant liquid was analysed for residual turbidity using the digital Lovibond turbidity meter. The results obtained for turbidity of sample in nephelometric turbidity units were converted to concentrations (mg/L) by multiplying with a factor of 2.3 [25].

4. Results and discussion

4.1. Effect of initial pH on % turbidity removal

Figs. 4(a) and 5(a) present the coagulation efficiency at various pH values for NaCl-extracted coagulant and KCL-extracted coagulant, respectively. At the end of 30 min of the coagulation process, we observed that the optimum conditions were 40 mL dosage and pH 7 for both the coagulants. Beyond neutral pH, the efficiency of the coagulation process decreased. It may

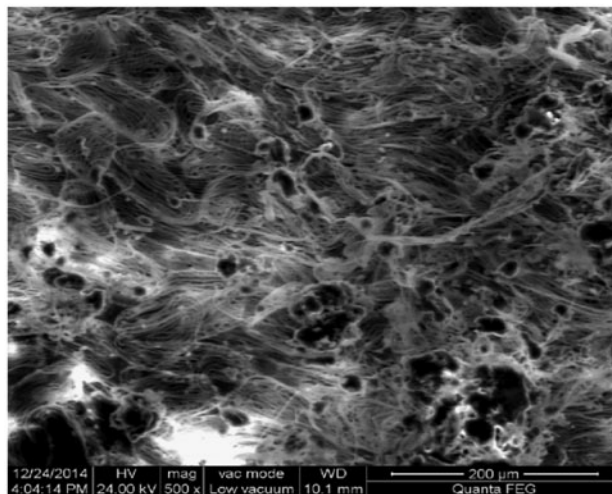


Fig. 3. SEM image of raw *M. oleifera* seed powder.

be due to the availability of OH^- ions at basic pH. These ions could increase the electrostatic repulsive coulombic force between the anions and colloidal impurities leading to the stability of the suspended impurities. At optimal conditions (pH 7 and 40 mL dosage), the turbidity removal efficiency of NaCl-extracted coagulant was 76.2%. This corresponds to the decrease in turbidity from 121.9 to 29.01 mg/L, which is lower than the recommended WHO limit of 30 mg/L [26]. The treated water turbidity value also complies with the discharge standard of 100 mg/L [27] specified by the Central Pollution Control Board,

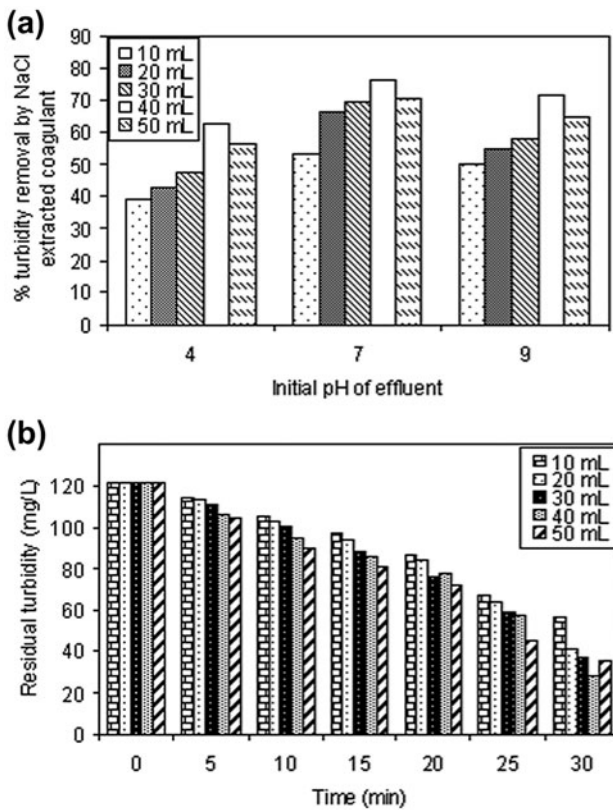


Fig. 4. Coagulation performance of NaCl-extracted coagulant as a function of (a) initial pH and (b) coagulation process time.

India. The maximum removal efficiency was 71.2% at the optimum operating condition for KCl-extracted coagulant. The removal efficiency of NaCl-extracted coagulant was more than KCl-extracted coagulant at the same optimum operating conditions.

Figs. 4(b) and 5(b) show the variation of residual turbidity as a function of process time for various

dosages of NaCl-extracted coagulant and KCl-extracted coagulant, respectively. Fig. 4(b) shows a linear decrease in turbidity concentration as time progresses and reaches a saturation limit beyond which the trend resembles a plateau showing no change in turbidity concentration.

It can be concluded that NaCl salt solution is better than the KCl salt solution in extracting active coagulating agent from *M. oleifera* seed powder. In coagulation, *M. oleifera* hardly affects the solution pH and conductivity [12]. Therefore, the wastewater treated with *M. oleifera* does not require chemicals for pH adjustment and the cost of chemicals are reduced.

4.2. Effect of coagulant dosage on removal efficiency

The effect of dosage on removal efficiency was studied by varying the coagulant dose at optimum pH (Fig. 6). NaCl-extracted coagulant showed better performance than KCl-extracted coagulant at all dosage levels. The optimum dosage was 40 mL (based on the variation of height of the rectangle in the bar chart). At this dosage, the % turbidity removal is the maximum which corresponds to optimal coagulant dosage. A decrease in efficiency was found beyond the optimum dosage and this could be attributed to increase in the zeta potential (measure of surface charge) of the suspended impurities. Another possible reason could be the increase in the kinetic energy due to Brownian motion of the suspended particles.

4.3. Coagulation process kinetics

In order to study the coagulation kinetics, residual particle concentration was measured as a function of time (Fig. 7). We observed that as time progresses,

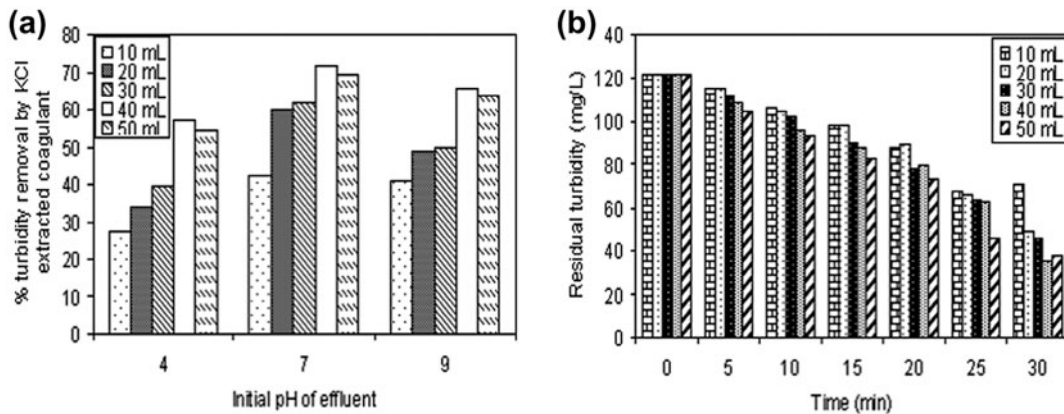


Fig. 5. Variation of turbidity removal efficiency by KCl-extracted coagulant with (a) initial pH and (b) coagulation process time.

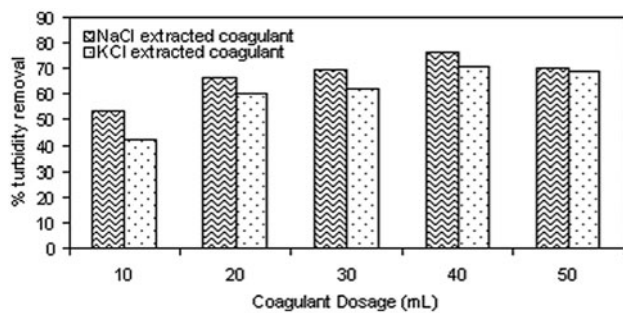


Fig. 6. Effect of coagulant dosage on removal efficiency for both coagulants at pH 7.

there was a decrease in turbidity concentration. The significance of this plot lies in the fact that the slope of the tangent line drawn at any point on the curve is equal to the rate of the coagulation process. The slope of the tangent line is negative due to the decreasing particle concentration with increasing time.

(slope of the tangent line at any point on the curve)

$$= (\text{rate of coagulation process}) = \frac{-dC}{dt} \tag{14}$$

The negative sign in the rate equation explains the decrease in turbidity concentration with increase in the time variable. The graph is nearly linear up to 15 min and then the slope decreases. The NaCl-extracted coagulant was efficient in reducing initial turbidity concentration than KCl-extracted coagulant within the process time range, and this conclusion is arrived since the trend graph for NaCl coagulant was below the trend graph for KCl-extracted coagulant. To

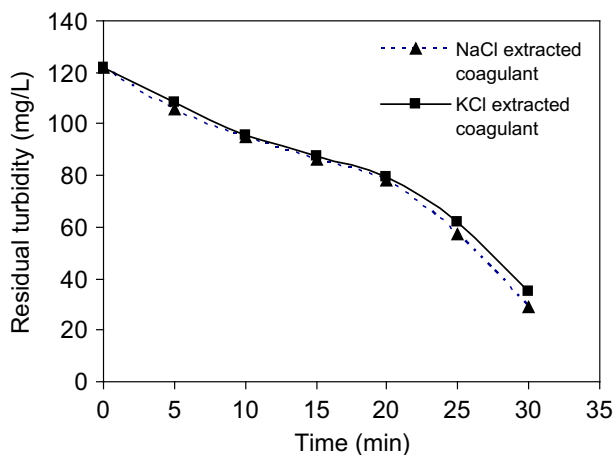


Fig. 7. Effect of process time on residual turbidity at initial pH 7 and 40 mL of coagulant dosage.

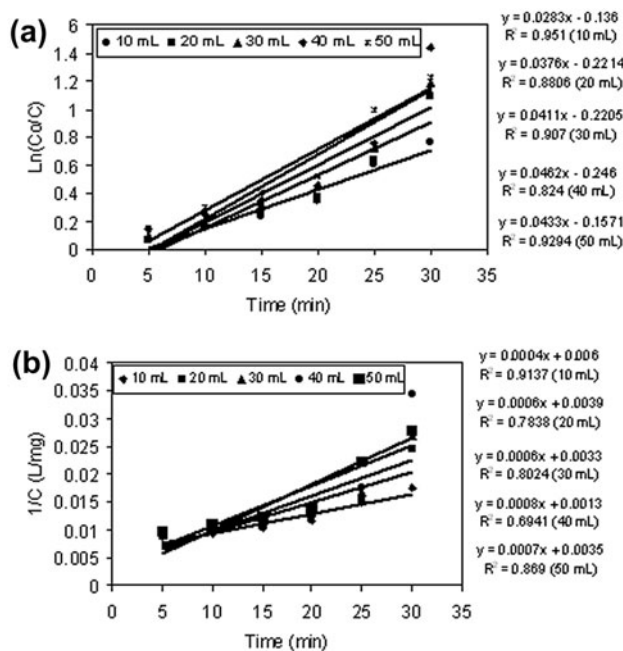


Fig. 8. Kinetic plots for NaCl-extracted coagulant dosages at pH 7 for (a) first-order process and (b) second-order process.

understand coagulation kinetics, the variation of residual turbidity with time for various coagulant dosages was studied. After 30 min of processing time, the residual turbidity was less at 40 mL dosage, which is the optimum dosage for maximum turbidity removal. It was established from the preliminary experiments that the time necessary for the coagulation process to attain an equilibrium condition is 30 min. The experiments which were performed beyond 30 min showed no significant change in residual turbidity concentration. In all the observed time concentration data, the residual turbidity of NaCl-extracted coagulant is less than KCl-extracted coagulant.

We used first-order process rate equation to test the experimental data and thus to explain the coagulation kinetics. For first-order kinetics, the integral form of rate equation is represented through Eq. (8). Fig. 8(a) shows the plot for such expression for various doses of NaCl-extracted coagulant. The experimental data did not fit the first-order kinetic model (the lines in the graph did not pass through the origin). Hence, the rate equation for second-order kinetics was considered and is explained by Eq. (10). Fig. 8(b) shows the concentration vs. time plot of such equation for NaCl-extracted coagulant. The plot of this graph is in agreement with second-order kinetic equation as it shows the Y-axis intercept. It should be noted that the coefficients of determination (R^2)

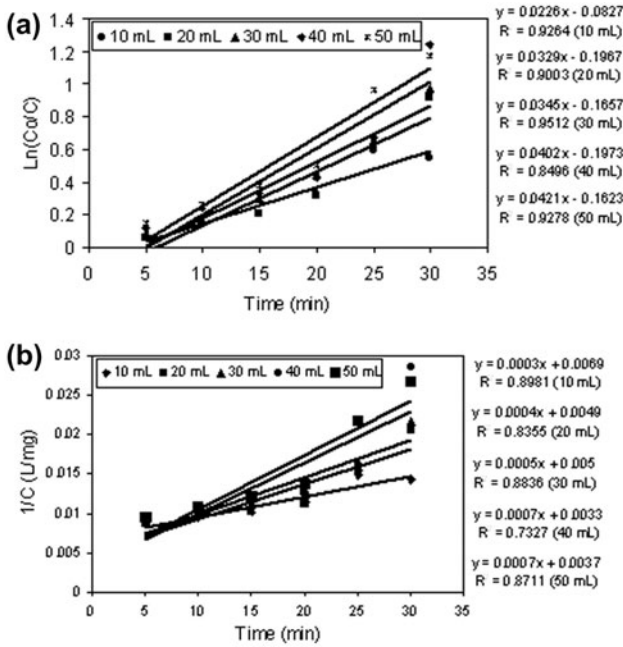


Fig. 9. Kinetic plots for KCl-extracted coagulant dosages at pH 7 for (a) first-order process and (b) second-order process.

obtained from the first- and the second-order plots reveal only the extent of linearity of the plots. At a low coagulant dosage (10 mL), the plot fits the experimental data with second-order kinetic model and is confirmed by high R^2 value. The second-order rate constant is 0.0004 L/(mg min), and the intercept made by regression line with the vertical Y-axis is 0.006 (L/mg). This intercept matches with the reciprocal value of initial turbidity which was 0.0082 (L/mg). This confirms the fact that second-order kinetic model best explains the rate of the coagulation process.

Fig. 9(a) shows the first-order kinetic plot for KCl-extracted coagulant. The coagulation process did not follow the first-order kinetics. The linear plot shown in Fig. 9(b) with intercept along Y-axis suggests that the coagulation process follows second-order kinetics similar to NaCl-extracted coagulant. The value of R^2 conforms the line of best fit which occurs at 10 mL dosage ($R^2 = 0.8981$). For NaCl- and KCl-extracted coagulant, the respective rate equations are:

$$\frac{1}{C} = 0.0004t + 0.006 \tag{15}$$

$$\frac{1}{C} = 0.0003t + 0.0069 \tag{16}$$

From Eqs. (15) and (16), we observed that the second-order rate constant for process based on NaCl-extracted coagulant is more in magnitude than KCl-extracted coagulant. We inferred that the rate of reduction in turbidity is faster for NaCl-based coagulant than KCl-extracted coagulant. The important functional and kinetic parameters of coagulation process were evaluated and presented in Tables 2–5 for both first- and second-order kinetics. The relationship between half-life period and initial turbidity concentration is given by the equation,

$$t_{1/2} \propto C_0^{1-n} \tag{17}$$

where “ n ” is the process order. From the tables, we observed that the half-life period decreases as the coagulant dose increases for the same initial turbidity. Eq. (13) was used to predict the growth of aggregating particles as a function of time for monomers ($m = 1$), dimmers ($m = 2$) and trimmers ($m = 3$), respectively.

Table 2
Functional and kinetic parameters for variable dosage of NaCl-extracted coagulant for various order reactions at pH 7

Process order	Parameter	10 mL	20 mL	30 mL	40 mL	50 mL
First order	R^2	0.9510	0.8806	0.9070	0.8240	0.9294
	k_1 (1/min)	0.0283	0.0376	0.0411	0.0462	0.0433
	β ($m^3/(kg\ s)$)	0.0566	0.0752	0.0822	0.0924	0.0866
	D ($kg^2/(m\ s)$)	7.3442×10^{-20}	5.5276×10^{-20}	5.0569×10^{-20}	4.4987×10^{-20}	4.8000×10^{-20}
	E	5.3103×10^{15}	7.0554×10^{15}	7.7121×10^{15}	8.6691×10^{15}	8.1249×10^{15}
	$(t_{1/2})_{I\text{order}}$ (min)	24.49	18.43	16.86	15.00	16.00
Second order	R^2	0.9137	0.7838	0.8024	0.6941	0.8690
	k_2 (lit/(mg min))	0.0004	0.0006	0.0006	0.0008	0.0007
	β ($m^3/kg\ s$)	0.0008	0.0012	0.0012	0.0016	0.0014
	D ($kg^2/m\ s$)	5.1960×10^{-18}	3.4640×10^{-18}	3.4640×10^{-18}	2.5980×10^{-18}	2.9691×10^{-18}
	E	7.5057×10^{13}	1.1258×10^{14}	1.1258×10^{14}	1.5011×10^{14}	1.3135×10^{14}
	$(t_{1/2})_{II\text{order}}$ (min)	20.51	13.67	13.67	10.25	11.72

Table 3

Functional and kinetic parameters for variable dosage of KCl-extracted coagulant for various order reactions at pH 7

Process order	Parameter	10 mL	20 mL	30 mL	40 mL	50 mL
First order	R^2	0.9264	0.9003	0.9512	0.8496	0.9278
	k_1 (1/min)	0.0226	0.0329	0.0345	0.0402	0.0421
	β ($\text{m}^3/(\text{kg s})$)	0.0452	0.0658	0.069	0.0804	0.0842
	D ($\text{kg}^2/(\text{m s})$)	9.1964×10^{-20}	6.3173×10^{-20}	6.0243×10^{-20}	5.1702×10^{-20}	4.9368×10^{-20}
	E	4.2407×10^{15}	6.1734×10^{15}	6.4737×10^{15}	7.5433×10^{15}	7.8998×10^{15}
	$(t_{1/2})_{\text{I order}}$ (min)	30.66	21.06	20.08	17.24	16.46
Second order	R^2	0.8981	0.8355	0.8836	0.7327	0.8711
	k_2 (lit/(mg min))	0.0003	0.0004	0.0005	0.0007	0.0007
	β ($\text{m}^3/\text{kg s})$	0.0006	0.0008	0.001	0.0014	0.0014
	D ($\text{kg}^2/\text{m s})$	6.9280×10^{-18}	5.1960×10^{-18}	4.1568×10^{-18}	2.9692×10^{-18}	2.9692×10^{-18}
	E	5.6293×10^{13}	7.5057×10^{13}	9.3822×10^{13}	1.3135×10^{13}	1.3135×10^{13}
	$(t_{1/2})_{\text{II order}}$ (min)	27.34	20.51	16.41	11.72	11.72

Table 4

Time growth of the cluster size distribution for 40 mL NaCl-extracted coagulant at pH 7

Parameter	Time (min)						
	0	5	10	15	20	25	30
Monomer particles count	121.9	78.79	55.08	40.66	31.25	24.76	20.09
Dimmer particles count	0	15.44	18.05	17.17	15.43	13.59	11.94
Trimmer particles count	0	3.03	5.92	7.26	7.62	7.47	7.09
Total particles	121.9	97.27	79.06	65.09	54.29	45.83	39.13

Table 5

Time growth of the cluster size distribution for 40 mL KCl-extracted coagulant at pH 7

Parameter	Time (min)						
	0	5	10	15	20	25	30
Monomer particles count	121.9	82.80	59.89	45.32	35.49	28.54	23.45
Dimmer particles count	0	14.55	17.91	17.68	16.34	14.73	13.17
Trimmer particles count	0	2.56	5.36	6.90	7.52	7.60	7.39
Total particles	121.9	99.92	83.16	69.91	59.35	50.88	44.00

The time evolution of the cluster size distribution for 40 mL dosage at pH 7 is shown in Fig. 10(a) and (b) for both types of coagulant. The curve trend is similar for all types of particle. The number of monomers decreases more rapidly than the total number of particles. The number of trimmers is the least among all types of particle. The destabilization of monomers facilitates the formation of dimmers and trimmers at a slow rate which is clearly indicated in the trend of the curve. Coagulation at pH 7 and dose 40 mL has the minimum $t_{1/2}$ value, suggesting very fast coagulation

rate. Therefore, at pH 7, very low hydrodynamic shear forces can cause flocculation to progress in a positive direction.

Fig. 11 shows the turbidity removal percentages using different coagulating agents. Experiments were carried out at pH 7 and varying dosage of each of the coagulants. Every product exhibited a slight removal activity with *M. oleifera* showing the highest removal efficiency. Alum and ferric chloride were used to compare the results from natural coagulants.

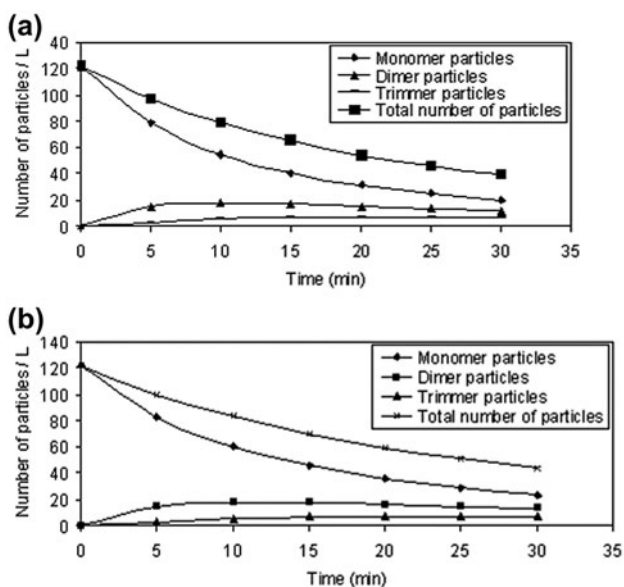


Fig. 10. Particle size distribution plot for 40 mL dosage at pH 7 of (a) NaCl-extracted coagulant and (b) KCl-extracted coagulant.

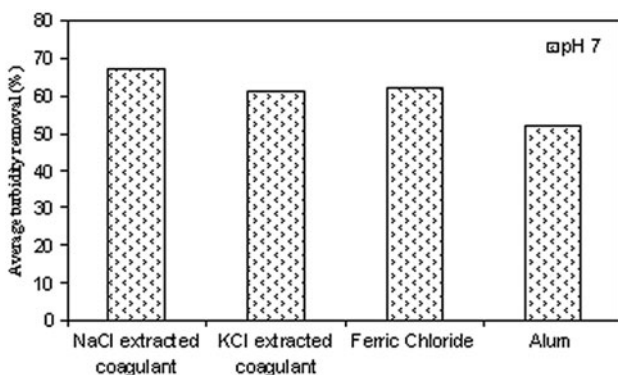


Fig. 11. Comparing turbidity removal efficiency by various coagulants at pH 7.

5. Conclusions

This study shows the scope of using *M. oleifera* seed protein as an effective organic coagulant in tannery wastewater treatment. The optimum turbidity removal was found at coagulant dosage 40 mL and pH 7 at the end of 30 min of coagulation for both NaCl- and KCl-extracted coagulants. The turbidity of the treated water was less than 30 mg/L, which corresponds with the removal of suspended and colloidal impurities. The coagulation process followed second-order kinetic equation for both extracted coagulants. The turbidity removal rate by NaCl-extracted coagulant was found to be more than the KCl-extracted

coagulant. Further, the flocs formed using NaCl-extracted coagulant settled at a faster rate compared with flocs using KCl-extracted coagulant. The second-order rate constants were 0.0004 (L/mg min) and 0.0003 (L/mg min), respectively, for both type coagulants. Coagulation capacity evaluated by the kinetic equation indicated that turbidity removal rate by NaCl-extracted coagulant was found to be more than the KCl-extracted coagulant.

List of symbols

K	—	process rate constant (1/min)
E	—	collision efficiency (dimensionless)
K_{RC}	—	Smoluchowski rate constant for rapid coagulation (1/min)
k_B	—	Boltzmann constant ($m^2 \text{ kg} / (s^2 \text{ K})$)
T	—	absolute temperature (K)
μ	—	viscosity of the effluent ($\text{kg} / (\text{m s})$)
β	—	friction factor due to shear stress ($\text{m}^3 / (\text{kg s})$)
D	—	Brownian diffusion coefficient ($\text{kg}^2 / (\text{m s})$)
C	—	turbid particle concentration in mg/L
t	—	coagulation process time (s)
n	—	order of the coagulation process

References

- [1] Z. Song, C.J. Williams, R.G.J. Edyvean, Treatment of tannery wastewater by chemical coagulation, *Desalination* 164 (2004) 249–259.
- [2] S. Aber, D. Salari, M.R. Parsa, Employing the Taguchi method to obtain the optimum conditions of coagulation–flocculation process in tannery wastewater treatment, *Chem. Eng. J.* 162(1) (2010) 127–134.
- [3] A. Amokrane, C. Comel, J. Veron, Landfill leachates pretreatment by coagulation–flocculation, *Water Res.* 31(11) (1997) 2775–2782.
- [4] R.A. Corbitt, H.B. Crawford, D. Gleason, *Standard Handbook of Environment Engineering*, McGraw Hill Publisher, New York, NY, 1989, pp. 671–698.
- [5] C.-Y. Yin, Emerging usage of plant-based coagulants for water and wastewater treatment, *Process Biochem.* 45 (2010) 1437–1444.
- [6] S. Vishali, R. Karthikeyan, *Cactus opuntia (ficus-indica)*: An eco-friendly alternative coagulant in the treatment of paint effluent, *Desalin. Water Treat.* (2014) 1–9, doi: 10.1080/19443994.2014.945487.
- [7] M.V. Jadhav, Y.S. Mahajan, Assessment of feasibility of natural coagulants in turbidity removal and modeling of coagulation process, *Desalin. Water Treat.* (2013) 1–10, doi: 10.1080/19443994.2013.816875.
- [8] L. Rizzo, G. Lofrano, V. Belgiorno, Olive mill and winery wastewaters pre-treatment by coagulation with chitosan, *Sep. Sci. Technol.* 45 (2010) 2447–2452.
- [9] S.M. Miller, E.J. Fugate, V.O. Craver, J.A. Smith, J.B. Zimmerman, Toward understanding the efficacy and mechanism of *Opuntia* spp. As a natural coagulant for potential application in water treatment, *Environ. Sci. Technol.* 42 (2008) 4274–4279.

- [10] S. Bhatia, Z. Othman, A.L. Ahmad, Coagulation–floculation process for POME treatment using *Moringa oleifera* seeds extract: Optimization studies, *Chem. Eng. J.* 133 (2007) 205–212.
- [11] S.A. Muyibi, C.A. Okuofu, Coagulation of low turbidity surface waters with *Moringa oleifera* seeds, *Int. J. Environ. Stud.* 48 (1995) 263–273.
- [12] A. Ndabigengesere, K.S. Narasiah, B.G. Talbot, Active agents and mechanism of coagulation of turbid waters using *Moringa oleifera*, *Water Res.* 29 (1995) 703–710.
- [13] A. Ndabigengesere, K.S. Subba Narasiah, Quality of water treated by coagulation using *Moringa oleifera* seeds, *Water Res.* 32(3) (1998) 781–791.
- [14] C.W. Goh, Effect of Room Temperature on Coagulation Performance of *Moringa oleifera* Seeds, B.Sc. Dissertation, Faculty of Engineering, Universiti Putra Malaysia, Serdang, Selangor, 2005.
- [15] M. Khayet, A.Y. Zahrim, N. Hilal, Modelling and optimization of coagulation of highly concentrated industrial grade leather dye by response surface methodology, *Chem. Eng. J.* 167 (2011) 77–83.
- [16] S. Haydar, J.A. Aziz, Characterization and treatability studies of tannery wastewater using chemically enhanced primary treatment (CEPT)—A case study of Saddiq Leather Works, *J. Hazard. Mater.* 163 (2009) 1076–1083.
- [17] R. Krishna Prasad, Color removal from distillery spent wash through coagulation using *Moringa oleifera* seeds: Use of optimum response surface methodology, *J. Hazard. Mater.* 165 (2009) 804–811.
- [18] J. Beltrán-Heredia, J. Sanchez Martin, M. Barrado Moreno, Long-chain anionic surfactants in aqueous solution. Removal by *Moringa oleifera* coagulant, *Chem. Eng. J.* 180 (2012) 128–136.
- [19] J.V.H. van Zanten, M. Elimelech, Determination of absolute coagulation rate constants by multiangle light scattering, *J. Colloid Interface Sci.* 154(1) (1992) 1–7.
- [20] J.U. Ani, N.J.N. Nnaji, O.D. Onukwuli, C.O.B. Okoye, Nephelometric and functional parameters response of coagulation for the purification of industrial wastewater using *Detarium microcarpum*, *J. Hazard. Mater.* 243 (2012) 59–66.
- [21] O. Levenspiel, *Chemical Reaction Engineering*, third ed., John Wiley & sons Inc., USA, 2011, p. 48.
- [22] A.E. Greenberg, *Standard Method for the Examination of Water and Wastewater*, eighteenth ed., APHA and AWWA, Washington DC, 1992.
- [23] S. Katayon, M.M. Noor, M. Asma, L.A. Ghani, A.M. Thamer, I. Azni, J. Ahmad, B.C. Khor, A.M. Suleyman, Effects of storage conditions of *Moringa oleifera* seeds on its performance in coagulation, *Bioresour. Technol.* 97(13) (2006) 1455–1460.
- [24] Y. Anjaneyulu, N.S. Sreedhara Chary, D.S.S. Samuel Suman Raj, Decolourization of industrial effluents—Available methods and emerging technologies—A Review, *Rev. Environ. Sci. Bio/Technol.* 4(4) (2005) 245–273.
- [25] G. Tchobanoglous, F.L. Burton, H.D. Stensel, *Wastewater Engineering, Treatment and Reuse*, Metcalf & Eddy Inc., Tata McGraw Hill, New Delhi, 2003.
- [26] N.J.N. Nnaji, J.U. Ani, L.E. Aneke, O.D. Onukwuli, U.C. Okoro, J.I. Ume, Modelling the coag–floculation kinetics of cashew nut testa tannins in an industrial effluent, *J. Ind. Eng. Chem.* 20(4) (2014) 1930–1935, doi: 10.1016/j.jiec.2013.09.013
- [27] <http://www.cpcb.nic.in/Industry-Specific-Standards/Effluent/418.pdf>.